Science and Technology Indonesia
e-ISSN:2580-4391 *p*-ISSN:2580-4405
Vol. 8, No. 3, July 2023

Research Paper

Coprecipitation Synthesis and Antimicrobial Effect Study of Europium Doped Spinel Manganese Ferrites Nanoparticles ($MnEu_{0.1}Fe_{1.9}O_4$NPs)

Amina Chidouh[1*], Tarek Tahraoui[2], Badra Barhouchi[3]

[1]*Laboratory of Chemistry, Physics and Materials Biology, Department of Natural Sciences, Higher Normal School of Technological Education, Skikda, 21000, Algeria*
[2]*Mines Metallurgy Materials Laboratory L3M, National Higher School of Technology and Engineering - ENSTI Annaba, 23000, Algeria*
[3]*Pharmaceutical Sciences Research Center (CRSP), Constantine, 25000, Algeria*
***Corresponding author**: amchidouh@gmail.com

Abstract
Due to the high prevalence of micro-organisms resistant to conventional antimicrobials, the search for new antimicrobial drugs is underway, with nanoparticles being one of the options. This study reports for the first time the use of the coprecipitation method to synthesize europium (Eu) doped spinel manganese ferrites nanoparticles ($MnEu_{0.1}Fe_{1.9}O_4$NPs). The purpose of this research is to determine the antimicrobial activity of $MnEu_{0.1}Fe_{1.9}O_4$NPs. $MnEu_{0.1}Fe_{1.9}O_4$NPs were analyzed using Fourier Transform Infrared Spectroscopy (FTIR), X-Ray Diffraction (XRD), and Scanning Electron Microscopy (SEM) combined with Energy Dispersive X-Ray Analysis (EDX) to determine their structure, size, morphology and elemental compositions. The antimicrobial activity of synthesized nanoparticles was evaluated qualitatively using a diffusion disc on agar, followed by minimum inhibitory concentrations (MIC) determination. The findings show that all tested strains were adversely affected by the examined NPs, where *E. coli* exhibited the highest sensitivity to NPs, followed by *S. aureus*. The NPs displayed a moderate level of anti-*candida* action. $MnEu_{0.1}Fe_{1.9}O_4$NPs could be exploited in biomedical usages.

Keywords
Coprecipitation Method, Nanoparticles, Antibacterial Activity, Anti-*candida* Action, Ferrites Spinel

Received: 19 January 2023, Accepted: 20 June 2023
https://doi.org/10.26554/sti.2023.8.3.494-500

1. INTRODUCTION

Antibacterial resistance rapidly increases throughout numerous bacterial species, becoming a significant clinical and public health problem worldwide (Kadiyala et al., 2018). Nanoscale engineering of nanoparticles (NPs) and surfaces gives new ways for antibacterial drugs that increase conventional organic chemistry methods (Bozon-Verduraz et al., 2009; Jiang et al., 2009). Metal oxide NPs (MO-NPs) have shown promising results in inhibiting bacterial growth and combating antibiotic resistance (Djurišić et al., 2015; Horie et al., 2012). MO-NPs are also desirable as antimicrobial medicaments because they are stable and less toxic to human cells than organic NPs (Deravi et al., 2007). Their nanoscale and variable surface chemistry. Their changeable surface chemistry and nanoscale permit MO-NPs to cause toxicity of bacteria over different modes of action, like proteolysis, enzyme inhibition, cell membrane lysis, oxidative stress and lipid peroxidation (Djurišić et al., 2015; Coker et al., 2012; Allahverdiyev et al., 2011).

Among the various MO-NPs, spinel ferrites (MFe_2O_4 such as M=Mn^{2+}, Fe^{2+}, Co^{2+}, Ni^{2+}) have been widely used due to their magnetic and electrical advantages (Reddy et al., 2012; Kollu et al., 2015). Mn is of particular interest in the biomedical field due to its different oxidation states. Mn^{2+} ions show the highest stability compared to Mn^{3+} and Mn^{4+} ions (Kalaiselvan et al., 2022). A cubic spinel structure characterizes manganese ferrite ($MnFe_2O_4$). These nanoparticles are necessary materials based on their moderate magnetization, size, biocompatibility, high sensitivity, good chemical stability and tunable toxicity in biological systems (Al Zahrani et al., 2022; Kalaiselvan et al., 2022).

These ferrites are highly important in biomedicine as magnetic carriers for bioseparation, protein immobilization and enzymes (Arulmurugan et al., 2005; Costa et al., 2003). $MnFe_2O_4$ nanostructures are promising for clinical cancer diagnosis and therapy (Kalaiselvan et al., 2022). The chemical formula AB_2O_4 generally represents the spinel structure, where A and B represent the tetrahedral (surrounded by 4 oxygen atoms) and octahedral (surrounded by 6 oxygen atoms) sites (Kalaiselvan et al., 2022).

Different synthesizing methods, such as hydrothermal synthesis, alcohol dehydration, and sol-gel and spray drying, have

been reported (Liu et al., 2018; Rahman and Ahmed, 2005). However, these processes are not economically suitable for large-scale production. The coprecipitation process enables the production of ultrafine powders with chemically uniform composition, orderly size and good reactivity (Bueno et al., 2007; Verma and Chatterjee, 2006). The advantages of this process are ease of processing, excellent production efficiency, low energy loss and high-purity product (Bandekar et al., 2019). The main drawbacks of co-precipitation methods are poor crystallinity and particle size dispersal, large agglomeration, and the need for pH control (Houshiar et al., 2014; Zahraei et al., 2015).

Recently, MO-NPs synthesized by rare earth (RE) ion doping have received considerable attention due to their field of applications (Park et al., 2016; Prodi et al., 2015; Wang, 2008). According to various studies (Bouzigues et al., 2011; Das and Das, 2013; Yu et al., 2009; Zhuang et al., 2015), rare-earth metals are essential in manufacturing modern technologies such as mobile phones, computers, biomedical applications and solar cells. Particular attention has been paid to rare-earth cations, such as Eu^{3+}, because of the resonance energy levels and their suited spectroscopic properties. Therefore, europium has been investigated for cancer treatment applications and used in dyes for magnetic resonance applications (Jahani et al., 2016). Rare earth elements doped manganese ferrite has many biological activities. Akhtar et al. (2019) concluded that $Mn_{0.5}Zn_{0.5}SmxEuxFe_{1.8-2x}O_4$ ($0.01 \leq x \leq 0.05$) NPs have potential probable anti-cancer and antibacterial abilities activities. Mohafez et al. (2021) indicated that an acceptable antifungal effect was observed in the presence of $MnCe_{1.4}Fe_{0.6}O_4$ nanoparticles. Al Zahrani et al. (2022) reported that the higher antibacterial activity of Ce^{3+} substituted $MnFe_2O_4$NCs was observed. Therefore, to our knowledge, there are currently undetailed studies about the synthesis and antimicrobial activity of europium-doped manganese ferrite nanoparticles ($MnEu_{0.1}Fe_{1.9}O_4$NPs). To this end, this study investigates an original study about the morphological, structural and antimicrobial activity of $MnEu_{0.1}Fe_{1.9}O_4$NPs. The findings that were achieved are thoroughly described.

2. EXPERIMENTAL SECTION

2.1 Synthesis of Europium-doped Manganese Ferrite Nano particles ($MnEu_{0.1}Fe_{1.9}O_4$NPs)

The coprecipitation method was used to synthesize nanoparticles of europium-doped manganese ferrite with the composition of $MnEu_{0.1}Fe_{1.9}O_4$NPs. Manganese chloride tetrahydrate $MnCl_2.4H_2O$ (Biochem, Chemopharma), europium chloride $EuCl_3$ (Sigma-Aldrich) and ferric chloride hexahydrate $FeCl_3.6H_2O$ (Biochem, Chemopharma) were taken in the molar ratio of 1:0.1:1.9 and dissolved in 100 mL of double-distilled water with constant magnetic stirring for an hour. Sodium hydroxide (2M) solution was added drop after drop until the solution's pH reached around 12. Instantaneously, the orange solution turned dark brown. The solution was stirred continuously in a water bath at 80°C. The precipitate was filtered and repeatedly rinsed with deionized water and acetone, then dehydrated at 80°C in the oven for 2 h. The sample was annealed at 600°C in an electric muffle furnace for 6h (Bandekar et al., 2019). The co-precipitated ferrite was ground using an agate pestle and mortar to obtain fine particles.

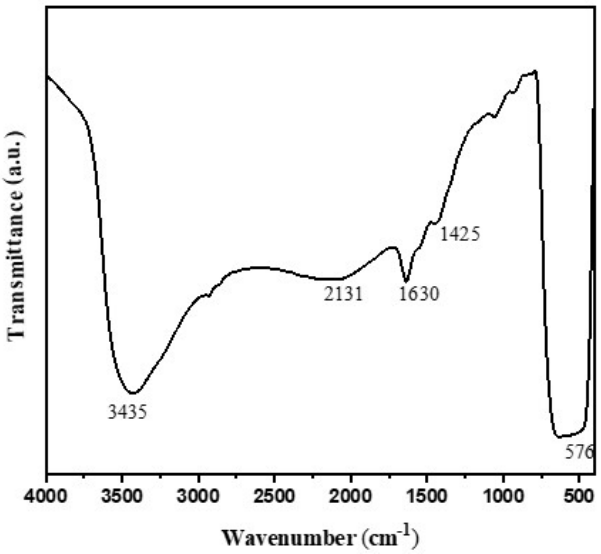

Figure 1. FTIR Spectrum of $MnEu_{0.1}Fe_{1.9}O_4$ Nanoparticles

2.1.1 $MnEu_{0.1}Fe_{1.9}O_4$NPs Characterization

Fourier Transform Infrared Spectroscopy (FTIR) analysis of the synthesized nanoparticles was obtained with a SHIMADZU FTIR-8000 spectrometer at room temperature utilizing KBr pellets in the range of frequency of 4000-400 cm^{-1} with a wavenumber resolution of 1 cm^{-1}. The morphological and elemental analysis was recorded using Scanning Electron Microscopy (SEM-EDX Quanta 250). X-ray Diffraction (XRD) analysis has been recorded utilizing a Rigaku X-ray diffractometer with high-intensity Cu-Kα radiation (λ = 1.54178 Å).

2.2 Microorganisms and Growth Conditions

This study utilized five classified bacteria ATCC: American Type Culture Collection: Gram-positive bacteria: *Staphylococcus aureus* 25923 and *Enterococcus faecalis* 29212, and Gram-negative bacteria: *Escherichia coli* 25922, *Klebsiella pneumoniae* 700603 and *Pseudomonas aeruginosa* 25953. One clinical yeast, *Candida albicans*, was also tested. The microorganisms were graciously supplied from the culture collection of the Pharmaceutical Sciences Research Center, Algeria. Nutrient agar was used as the growth media.

2.3 Antimicrobial Assays

The qualitative assessment of the synthesized nanoparticles antimicrobial effect was performed using disk diffusion on agar and minimum inhibitory concentration (MIC) (Vanden and Vlirtinck, 1993). The microbial strains were pre-grown at

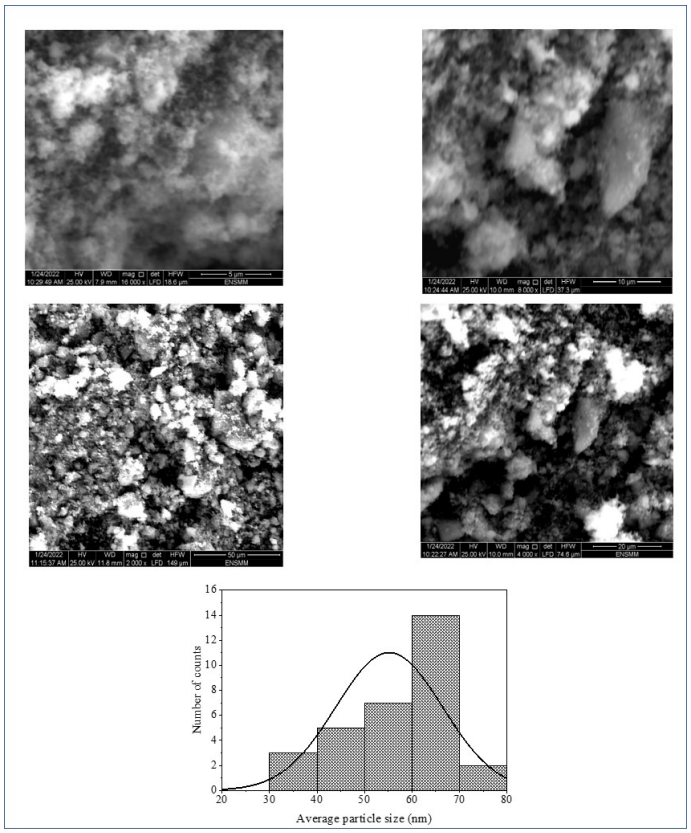

Figure 2. SEM Micrographs with Average Particle Size Distribution of $MnEu_{0.1}Fe_{1.9}O_4$

Table 1. Elemental Composition of $MnEu_{0.1}Fe_{1.9}O_4$ Nanoparticles Obtained from EDX Analysis

Elements	Weight%	Atomic%
O K	47.89	77.28
EuL	5.08	0.86
MnK	15.48	7.27
FeK	31.55	14.59

37.0±0.1°C for 18 h on nutrient agar. Each strain was diluted in a saline solution at the McFarland scale 0.5, 1.5×10^8 UFC/mL (equivalent to DO 0.08-0.1/λ = 625 nm). The inoculum was streaked into agar plates using a sterile swab after the Mueller Hinton Agar (MHA) had solidified, and the surface of the MHA was covered with a sterile filter disc (Whatman paper N°3) with a 6-mm diameter. A concentration of 2 mg/mL of NPs was prepared in methanol, and 50 μL of the NPs was dropped onto the inserted discs. The plates have been kept at 37°C for 18-24 h. Methanol was employed as a negative control. Gentamicin (GEN) and ampicillin (AMP) were used as positive controls. The effectiveness was determined by determining the zone's diameter of microbial growth inhibition (ZOI) atop the disc and recording the diameter with a transparent ruler in millimeters. All tests were performed in triplicate.

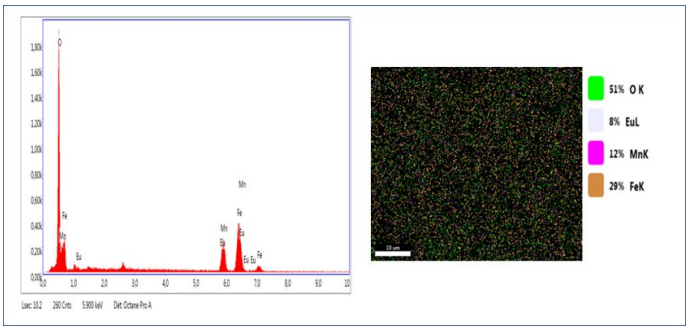

Figure 3. EDX Spectra and Elemental Composition for $MnEu_{0.1}Fe_{1.9}O_4$ Nanoparticles

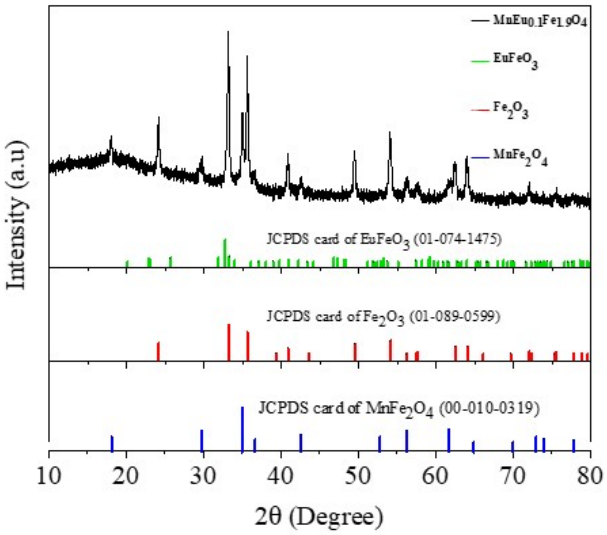

Figure 4. XRD Pattern of $MnEu_{0.1}Fe_{1.9}O_4$ Nanoparticles

MIC experiment was done in the 96-microplate using the broth dilution method. 100 μL volume of the obtained nanoparticle at different concentrations (16 to 0.5 mg/mL) was prepared in wells previously inoculated with 50 μL of Mueller Hinton Broth (MHB) broth medium. The freshly adjusted inoculum to DO of 0.08 to 0.1 (50 μL) was added to the prepared NPs solution and then incubated for 24 hours at 37°C. Untreated bacteria with DMSO was used in the trial as the negative control. The lowest concentration of the tested compound that the microorganism does not demonstrate visible growth was defined as the minimum inhibitory concentration (MIC) (Rehman et al., 2019).

3. RESULTS AND DISCUSSION

FTIR Spectroscopy is a valuable technique for structural analysis and cations redistribution between tetrahedral and octahedral sites in spinel structures (Hakeem et al., 2016). Figure 1 shows the FTIR spectrum of $MnEu_{0.1}Fe_{1.9}O_4$NPs. The band at 1425 cm^{-1} is for out-of-plane deformation vibration of the C-H. A band characterizes adsorbed water at 3435 cm^{-1}. The

bands at 2131 cm^{-1} and 1630 cm^{-1} are attributed to O-H stretching and H-O-H bonded vibration modes, respectively. The existence of the 576 cm^{-1} band is based on the vibration stretching of octahedral and tetrahedral groups (Hakeem et al., 2016).

Figure 2 shows the Scanning Electron Microscopy (SEM) micrographs of $MnEu_{0.1}Fe_{1.9}O_4$ NPs. Micrographs were taken at scales of 5, 10, 20 and 50 µm, it demontrates the formation with uniform distribution of agglomerated nanoparticles (Devi and Soibam, 2018). Due to their high surface energy and magnetic properties, nanoparticles have the potential to aggregate and develop into large assemblages (Sagadevan et al., 2018). The average nanoparticles size distribution was estimated in the range of (30 nm-70 nm) using imageJ software .

Figure 3 displays the results of EDX measurments for the elemental composition of the prepared sample. EDX spectra show the purity, homogeneity and presence of Eu in the sample, indicating that Eu was successfully doped into the spinel structure. As determined by the EDX analyses, the elemental composition is listed in Table 1 with the atomic and weight percentages.

X-ray diffraction measurements show that peaks of $MnEu_{0.1}Fe_{1.9}O_4$NPs correspond to peaks of a typical spinel structure prepared by coprecipitation. Figure 4 displays the prepared nanoparticles X-ray Diffraction pattern. The crystallite's average size was in the range of 40.9 nm. Intense diffraction peaks occur at 2θ=18.15°, 29.78°, 34.99°, 42.63°, 52.70°, 56.18°, 61.73°, 64.68° corresponds to (111), (220), (311), (400), (422), (511), (440), (531) usual planes of ferrite spinel arrangements Fe_2MnO_4 that is characterized by face-centered cubic phase belonging to space group of Fd3m (Hakeem et al., 2016; Mohafez et al., 2021) according to the standard card JCPDS file no. 100319 (Wang, 2008). It is observed at about (20.24°, 33.25° and 40.90°) and (24.22°, 33.25°, 35.68°, 49.57° and 54.26°) the appearance of secondary phase peaks with an insignificant amount which corresponds to the ortho ferrite ($EuFeO_3$) (01-074-1475) and hematite (Fe_2O_3) (01-089-0599) phases respectively (Zubair et al., 2017).

One of the crucial causes in the development of secondary phases is attributed to the low solubility and electronic configuration of the rare earth element Eu^{3+} (Mohafez et al., 2021; Shirsath et al., 2014). The Eu^{3+} ion with a bigger radius of about (1.07 Å) prefers to occupy the octahedral sites of Fe^{3+}, whose ionic radius is 0.67 Å. Consequently, when the Eu^{3+} ions substitution is high, this directs to the creation of secondary phases as an impurity on the grain boundaries due to the diffusion of RE-Eu^{3+} ions (Zubair et al., 2017). The sample's average value of the peaks of XRD analysis is used to determine the crystallite size (D). The value of 'D' is calculated using Scherrer's formula Cullity (1978) as follows:

$$D = K\beta\cos\theta \quad (1)$$

In which 'D' signifies the average crystallite size in nm, the shape factor, 'k', has a value of 0.94, X-rays are employed, and their wavelength is λ, θ is the Bragg's diffraction angle, and β is FWHM (Zubair et al., 2017).

To the best of our knowledge, the antimicrobial action of $MnEu_{0.1}Fe_{1.9}O_4$NPs was investigated for the first time on both yeast and Gram-positive/negative bacteria. Subsequently, the results indicate that the synthesized $MnEu_{0.1}Fe_{1.9}O_4$NPs had exceptional antimicrobial activity against selected microbial strains as shown in Table 2. Moreover, the checked NPs were harmful to all the tested strains at the dose of 2 mg/mL and gave moderate to strong activity, which indicated by the formation of a clear zone. The inhibition zones (ZOI) were ranged from 12 to 24 mm. Among the tested bacterial strains, *E. coli* exhibited the strongest sensitivity to NPs, followed by *S. aureus*, with ZOI values of 24 ± 0.14 mm and 21 ± 0.24 mm, respectively. Furthermore, the produced NPs also displayed an equally positive effect against *E. faecalis*, *K. pneumoniae* and *P. aeruginosa*. Xiu et al. (2012) included that inorganic nanoparticles are distinguished for their large surface-to-volume ratios and nanoscale sizes, enhancing their response to pathogenic bacteria. According to Jesudoss et al. (2016), the ferrite nanoparticles involved significantly in combating infectious against both Gram-positive and Gram-negative bacteria.

In addition, *Candida albicans* remains a potent yeast strain, where the NPs showed a moderate anti-*candida* activity and presented the weakest inhibition zone (ZOI: 12 ± 0.24 mm). The encouraging antibacterial potential of $MnEu_{0.1}Fe_{1.9}O_4$NPs nanoparticles was corroborated by the results of experiments and compared with antibiotics, gentamicin and ampicillin, as a positive control. Contrary to gentamicin which displayed a remarkable antibacterial activity, ampicillin had no effect against all tested bacteria. As revealed in Table 2, the MIC (minimum inhibitory concentration) of $MnEu_{0.1}Fe_{1.9}O_4$NPs was found to be 1 mg/mL for *E. coli*, *K. pneumoniae*, *P. aeruginosa* and *C. albicans* whereas 2 mg/mL MIC value was recorded for *S. aureus* and *E. faecalis*. In agreement with our results, the synthesized europium doped cerium dioxide ($Eu^{3+}CeO_2$) nanoparticles exhibited outstanding antibacterial effectiveness against *E. coli* and *S. aureus* with the following diameter of inhibition zone (ZOI): 37 ± 0.3 mm and 18 ± 0.2 mm, respectively (Gnanam et al., 2021). Ashour et al. (2018) demonstrated that the ferrites had antibacterial activity against all pathogens tested. Zinc cobalt ferrite nanoparticles (ZCFO) were the most effective, with zones of inhibition of 13.0 mm against *Bacillus subtilis* and *Staphylococcus aureus*.

However, Akhtar et al. (2019) demonstrated an improved activity against *E. coli* compared with *S. aureus* of $Mn_{0.5}Zn_{0.5}Sm_xEu_xFe_{1.8-2x}O_4$NPs. In contrast, Mohafez et al. (2021) concluded that $MnFe_2O_4$ and $MnCe_{1.4}Fe_{0.6}O_4$NP s did not show antibacterial activity against infectious Gram-negative bacteria: (*Escherichia coli*, *Acinetobacter baumannii* and *Pseudomonas aeruginosa*), as well as infectious Gram-positive bacteria: (*Bacillus cereus*, *Staphylococcus epidermidis* and *Streptococcus pneumoniae*) even at concentrations of 1024 $\mu g\ mL^{-1}$. According to

Table 2. Antimicrobial Activity of $MnEu_{0.1}Fe_{1.9}O_4$NPs Tested Against Various Microorganisms

Microbial Strains	Reference Number (ATCC)	Zone of Inhibition ZOI (mm)				MIC (mg/mL)
		$MnEuFe_2O_4$	Gentamicina	Ampicillina	Methanolb	
E. coli	25922	24± 0.14	20± 0.23	-	-	1
S. aureus	25923	21± 0.24	23± 0.29	-	-	2
K. pneumoniae	700603	15± 0.32	11± 0.30	-	-	1
P. aeruginosa	25953	15± 0.15	15± 0.12	-	-	1
E. faecalis	29212	15± 0.33	20± 0.29	-	-	2
C. albicans	Clinical	12± 0.24	/	/	-	1

ATCC: American Type Culture collection (a): Positive control (Antibiotics: Gentamicin GEN and Ampicillin AMP), (b): Negative control (Methanol), (-): No effect.MIC: minimum inhibitory concentration of the tested NPs. The results were expressed as mean ± standard deviation.

Gheidari et al. (2020), *Pseudomonas aeruginosa* and *Staphylococcus aureus* were the most resistant bacteria against $CoFe_2O_4$ nanoparticles.

$MnFe_2O_4$ and $MnCe_{1.4}Fe_{0.6}O_4$ nanoparticles were also tested against pathogenic fungi *Aspergillus fumigatus*, *Candida albicans* and *Fusarium oxysporum*. As a result, adequate antifungal activities were detected in the presence of $MnCe_{1.4}Fe_{0.6}O_4$ nanoparticles (Mohafez et al., 2021). Al Zahrani et al. (2022) showed that the increasing concentrations of $MnFe_2O_4$ and Ce-doped $MnFe_2O_4$ nanocrystallites (NCs) eventually stop the replication operation and cease the spread of Gram-negative/positive bacterium when the $MnCe_{0.3}Fe_{1.7}O_4$NCs had higher activity than the other doped and undoped samples. Meanwhile, the bacterial status and inoculum size influenced the effectiveness of antimicrobials as well as their applied concentrations (Li et al., 2017). However, our findings showed that our $MnEu_{0.1}Fe_{1.9}O_4$NPs has a better antibacterial effect against Gram-negative bacteria. It could be because this class of bacteria has less rigid cell walls than Gram-positive bacteria, which have a more complicated outer membrane (Jiang et al., 2020). Generally, their cell wall is thicker due to the peptidoglycan layer absent in Gram-negative bacteria. This layer hinders the penetration of metal ions into the cytoplasm, whereas in Gram-negative bacteria, the NPs easily penetrate the cell membrane and cause damage (Slavin et al., 2017). The improved antibacterial action might be associated with the exposure of ions that have positive charges, like as Eu^{3+}, Fe^{3+} and Mn^{2+}, which charge the bacteria membrane and affect membrane wholeness, therefore, can decrease electrostatic interaction, allowing membrane obstacles to be traversed, which disturbs the respiratory chain that kills cells. Cell death is brought on by breaching membrane barriers, which messes up the electron transport chain (Al Zahrani et al., 2022). Thus, the reported antimicrobial property of $MnEu_{0.1}Fe_{1.9}O_4$NPs in this research will open up a new way to apply these nanoparticles as a new source of antimicrobials, which can be further explored in the biomedical sector.

4. CONCLUSION

Spinel europium-doped manganese ferrite nanoparticles ($MnEu_{0.1}Fe_{1.9}O_4$NPs) were synthesized using coprecipitation method. By using XRD analysis, the sample's spinel cubic structure was determined. The crystallite's average size was in the range of 40.9 nm. EDX spectra of the sample confirm the successful doping of Eu into the spinel structure. The antimicrobial action of $MnEu_{0.1}Fe_{1.9}O_4$NPs was investigated on both yeast and Gram-positive/negative bacteria. The present study showed that the synthesized $MnEu_{0.1}Fe_{1.9}O_4$NPs had exceptional antimicrobial activity against selected microbial strains and can be used in biomedical applications.

5. ACKNOWLEDGMENT

We are grateful to Professor Djekoun Abdelhamid, the Director of Pharmaceutical Sciences Research Center (CRSP), Algeria for his support. We respectfully acknowledge the contribution made to this research by Dr. Boukhzar Skander, Research fellow at the Research Center in Industrial Technologies (CRTI), Algeria.

REFERENCES

Akhtar, S., S. Rehman, M. A. Almessiere, F. A. Khan, Y. Slimani, and A. Baykal (2019). Synthesis of $Mn_{0.5}Zn_{0.5}S_{mx}Eu_xFe_{1.8-2x}O_4$ Nanoparticles Via the Hydrothermal Approach Induced Anti-cancer and Antibacterial Activities. *Nanomaterials*, **9**(11); 1635

Al Zahrani, S. A., A. Manikandan, K. Thanrasu, A. Dinesh, K. K. Raja, M. Almessiere, Y. Slimani, A. Baykal, S. Bhuminathan, and S. R. Jayesh (2022). Influence of Ce^{3+} on the Structural, Morphological, Magnetic, Photocatalytic and Antibacterial Properties of Spinel MnFe2O4 Nanocrystallites Prepared by the Combustion Route. *Crystals*, **12**(2); 268

Allahverdiyev, A. M., K. V. Kon, E. S. Abamor, M. Bagirova, and M. Rafailovich (2011). Coping with Antibiotic Resistance: Combining Nanoparticles with Antibiotics and Other Antimicrobial Agents. *Expert Review of Anti-infective Therapy*, **9**(11); 1035–1052

Arulmurugan, R., B. Jeyadevan, G. Vaidyanathan, and S. Sendhilnathan (2005). Effect of Zinc Substitution on Co–Zn and Mn–Zn Ferrite Nanoparticles Prepared by Co-precipitation. *Journal of Magnetism and Magnetic Materials*, **288**; 470–477

Ashour, A., A. I. El Batal, M. A. Maksoud, G. S. El Sayyad, S. Labib, E. Abdeltwab, and M. El Okr (2018). Antimicrobial Activity of Metal-substituted Cobalt Ferrite Nanopar-

ticles Synthesized by sol–gel Technique. *Particuology*, **40**; 141–151

Bandekar, A. S., P. S. Gaikar, A. P. Angre, A. M. Chaughule, and N. S. Pradhan (2019). Effect of Annealing on Microstructure and Magnetic Properties of Mn Ferrite Powder. *Journal of Biological and Chemical Chronicles*, **5**(3); 74–78

Bouzigues, C., T. Gacoin, and A. Alexandrou (2011). Biological Applications of Rare-earth Based Nanoparticles. *ACS nano*, **5**(11); 8488–8505

Bozon-Verduraz, F., F. Fiévet, J. Y. Piquemal, R. Brayner, K. El Kabouss, Y. Soumare, G. Viau, and G. Shafeev (2009). Nanoparticles of Metal and Metal Oxides: Some Peculiar Synthesis Methods, Size and Shape Control, Application to Catalysts Preparation. *Brazilian Journal of Physics*, **39**; 134–140

Bueno, A. R., M. L. Gregori, and M. C. Nóbrega (2007). Effect of Mn Substitution on the Microstructure and Magnetic Properties of $Ni_{0.50-x}Zn_{0.50-x}Mn_{2x}Fe_2O_4$ Ferrite Prepared by the Citrate–nitrate Precursor Method. *Materials Chemistry and Physics*, **105**(2-3); 229–233

Coker, V. S., M. Green, and S. A. Corr (2012). *Nanoscience: Volume 1: Nanostructures Through Chemistry*, volume 1. Royal Society of Chemistry

Costa, A., E. Tortella, M. Morelli, and R. Kiminami (2003). Synthesis, Microstructure and Magnetic Properties of Ni–Zn Ferrites. *Journal of Magnetism and Magnetic Materials*, **256**(1-3); 174–182

Cullity, B. (1978). *Element of X-Ray Diffraction 2nd Edition*. United States of America: Addison-WesleyPublishing CompanyInc

Das, N. and D. Das (2013). Recovery of Rare Earth Metals Through Biosorption: An Overview. *Journal of Rare Earths*, **31**(10); 933–943

Deravi, L. F., J. D. Swartz, and D. W. Wright (2007). *The Biomimetic Synthesis of Metal Oxide Nanomaterials*. Wiley-VCH Verlag GmbH & Co. KGaA Weinheim, Germany

Devi, E. C. and I. Soibam (2018). A Facile Low-Temperature Synthesis of $MnLa_xFe_{2-x}O_4$ Nanoferrites with Structural and Electrical Characterization. *Journal of Superconductivity and Novel Magnetism*, **31**; 1615–1621

Djurišić, A. B., Y. H. Leung, A. M. Ng, X. Y. Xu, P. K. Lee, N. Degger, and R. Wu (2015). Toxicity of Metal Oxide Nanoparticles: Mechanisms, Characterization, and Avoiding Experimental Artefacts. *Small*, **11**(1); 26–44

Gheidari, D., M. Mehrdad, S. Maleki, and S. Hosseini (2020). Synthesis and Potent Antimicrobial Activity of $CoFe_2O_4$ Nanoparticles Under Visible Light. *Heliyon*, **6**(10); 05058

Gnanam, S., J. Gajendiran, J. R. Ramya, K. Ramachandran, and S. G. Raj (2021). Glycine Assisted Hydrothermal Synthesis of Pure and Europium Doped CeO_2 Nanoparticles and Their Structural, Optical, Photoluminescence, Photocatalytic and Antibacterial Properties. *Chemical Physics Letters*, **763**; 138217

Hakeem, A., G. Murtaza, I. Ahmad, P. MAOc, X. Guohua, M. Farid, M. Kanwal, G. Mustafa, M. Hussain, and M. Ahmad (2016). Effect Of Multiwalled Carbon Nanotubes on Co-Mn Ferrite Prepared by Co-precipitation Technique. *Digest Journal of Nanomaterials and Biostructures*, **11**; 149–157

Horie, M., K. Fujita, H. Kato, S. Endoh, K. Nishio, L. K. Komaba, A. Nakamura, A. Miyauchi, S. Kinugasa, and Y. Hagihara (2012). Association of the Physical and Chemical Properties and the Cytotoxicity of Metal Oxidenanoparticles: Metal Ion Release, Adsorption Ability and Specific Surface Area. *Metallomics*, **4**(4); 350–360

Houshiar, M., F. Zebhi, Z. J. Razi, A. Alidoust, and Z. Askari (2014). Synthesis of Cobalt Ferrite ($CoFe_2O_4$) Nanoparticles Using Combustion, Coprecipitation, and Precipitation Methods: A Comparison Study of Size, Structural, and Magnetic Properties. *Journal of Magnetism and Magnetic Materials*, **371**; 43–48

Jahani, S., M. Khorasani Motlagh, and M. Noroozifar (2016). DNA Interaction of Europium(III) Complex Containing 2, 2'-Bipyridine and Its Antimicrobial Activity. *Journal of Biomolecular Structure and Dynamics*, **34**(3); 612–624

Jesudoss, S., J. J. Vijaya, L. J. Kennedy, P. I. Rajan, H. A. Al Lohedan, R. J. Ramalingam, K. Kaviyarasu, and M. Bououdina (2016). Studies on the Efficient Dual Performance of $Mn_{1-x}NixFe_2O_4$ Spinel Nanoparticles in Photodegradation and Antibacterial Activity. *Journal of Photochemistry and Photobiology B: Biology*, **165**; 121–132

Jiang, L., Y. Wen, Z. Zhu, C. Su, S. Ye, J. Wang, X. Liu, and W. Shao (2020). Construction of an Efficient Nonleaching Graphene Nanocomposites with Enhanced Contact Antibacterial Performance. *Chemical Engineering Journal*, **382**; 122906

Jiang, W., H. Mashayekhi, and B. Xing (2009). Bacterial Toxicity Comparison Between Nano-and Micro-scaled Oxide Particles. *Environmental pollution*, **157**(5); 1619–1625

Kadiyala, U., N. A. Kotov, and J. S. VanEpps (2018). Antibacterial Metal Oxide Nanoparticles: Challenges in Interpreting the Literature. *Current Pharmaceutical Design*, **24**(8); 896–903

Kalaiselvan, C. R., S. S. Laha, S. B. Somvanshi, T. A. Tabish, N. D. Thorat, and N. K. Sahu (2022). Manganese Ferrite ($MnFe_2O_4$) Nanostructures for Cancer Theranostics. *Coordination Chemistry Reviews*, **473**; 214809

Kollu, P., P. R. Kumar, C. Santosh, D. K. Kim, and A. N. Grace (2015). A High Capacity $MnFe_2O_4$/rGO Nanocomposite for Li and Na-ion Battery Applications. *RSC Advances*, **5**(78); 63304–63310

Li, J., S. Xie, S. Ahmed, F. Wang, Y. Gu, C. Zhang, X. Chai, Y. Wu, J. Cai, and G. Cheng (2017). Antimicrobial Activity and Resistance: Influencing Factors. *Frontiers in Pharmacology*, **8**; 364

Liu, S., L. Wang, and K. Chou (2018). Synthesis of Metal-doped Mn-Zn Ferrite from the Leaching Solutions of Vanadium Slag Using Hydrothermal Method. *Journal of Magnetism and Magnetic Materials*, **449**; 49–54

Mohafez, F. S., A. M. Davarpanah, A. Rahdar, H. Beyzaei, O. Zeybek, and S. Barrett (2021). Structural, Magnetic,

and in Vitro Inhibitory Characteristics of Ce-substituted $MnFe_2O_4$ Nanoparticles. *Applied Physics A*, **127**; 1–7

Park, J. C., S. Yeo, M. Kim, G. T. Lee, and J. H. Seo (2016). Synthesis and Characterization of Novel Lanthanide-doped Magnetite@ Au core@ Shell Nanoparticles. *Materials Letters*, **181**; 272–277

Prodi, L., E. Rampazzo, F. Rastrelli, A. Speghini, and N. Zaccheroni (2015). Imaging Agents Based on Lanthanide Doped Nanoparticles. *Chemical Society Reviews*, **44**(14); 4922–4952

Rahman, I. and T. Ahmed (2005). A Study on Cu Substituted Chemically Processed Ni–Zn–Cu Ferrites. *Journal of Magnetism and Magnetic Materials*, **290**; 1576–1579

Reddy, L. H., J. L. Arias, J. Nicolas, and P. Couvreur (2012). Magnetic Nanoparticles: Design and Characterization, Toxicity and Biocompatibility, Pharmaceutical and Biomedical Applications. *Chemical Reviews*, **112**(11); 5818–5878

Rehman, S., S. M. Asiri, F. A. Khan, B. R. Jermy, H. Khan, S. Akhtar, R. A. Jindan, K. M. Khan, and A. Qurashi (2019). Biocompatible Tin Oxide Nanoparticles: Synthesis, Antibacterial, Anticandidal and Cytotoxic Activities. *Chemistry Select*, **4**(14); 4013–4017

Sagadevan, S., Z. Z. Chowdhury, and R. F. Rafique (2018). Preparation and Characterization of Nickel Ferrite Nanoparticles Via Co-precipitation Method. *Materials Research*, **21**

Shirsath, S. E., M. L. Mane, Y. Yasukawa, X. Liu, and A. Morisako (2014). Self-ignited High Temperature Synthesis and Enhanced Super-exchange Interactions of Ho^{3+}-Mn^{2+}-Fe^{3+}-O^{2-} Ferromagnetic Nanoparticles. *Physical Chemistry Chemical Physics*, **16**(6); 2347–2357

Slavin, Y. N., J. Asnis, U. O. Hńfeli, and H. Bach (2017). Metal Nanoparticles: Understanding the Mechanisms Behind Antibacterial Activity. *Journal of Nanobiotechnology*, **15**; 1–20

Vanden, D. and A. Vlirtinck (1993). Screening Methods for Antibacterial Agents From Higher Plants. *Methods in Plant Biochemistry. 4th ed, Elsevier Ltd*, **10**; 1–297

Verma, A. and R. Chatterjee (2006). Effect of Zinc Concentration on the Structural, Electrical and Magnetic Properties of Mixed Mn–Zn and Ni–Zn Ferrites Synthesized by the Citrate Precursor Technique. *Journal of Magnetism and Magnetic Materials*, **306**(2); 313–320

Wang, W. W. (2008). Microwave Induced Polyol-process Synthesis of $M_{II}Fe_2O_4$ (M= Mn, Co) Nanoparticles and Magnetic Property. *Materials Chemistry and Physics*, **108**(2-3); 227–231

Xiu, Z. m., Q. b. Zhang, H. L. Puppala, V. L. Colvin, and P. J. Alvarez (2012). Negligible Particle-specific Antibacterial Activity of Silver Nanoparticles. *Nano letters*, **12**(8); 4271–4275

Yu, M., F. Li, Z. Chen, H. Hu, C. Zhan, H. Yang, and C. Huang (2009). Laser Scanning Up-conversion Luminescence Microscopy for Imaging Cells Labeled with Rare-earth Nanophosphors. *Analytical Chemistry*, **81**(3); 930–935

Zahraei, M., A. Monshi, M. del Puerto Morales, D. Shahbazi Gahrouei, M. Amirnasr, and B. Behdadfar (2015). Hydrothermal Synthesis of Fine Stabilized Superparamagnetic Nanoparticles of Zn2+ Substituted Manganese Ferrite. *Journal of Magnetism and Magnetic Materials*, **393**; 429–436

Zhuang, W. Q., J. P. Fitts, C. M. Ajo Franklin, S. Maes, L. Alvarez Cohen, and T. Hennebel (2015). Recovery of Critical Metals Using Biometallurgy. *Current Opinion in Biotechnology*, **33**; 327–335

Zubair, A., Z. Ahmad, A. Mahmood, W. C. Cheong, I. Ali, M. A. Khan, A. H. Chughtai, and M. N. Ashiq (2017). Structural, Morphological and Magnetic Properties of Eu Doped $CoFe_2O_4$ Nano-ferrites. *Results in Physics*, **7**; 3203–3208

